Rail Vehicles/Pojazdy Szynowe

www.railvehicles.eu

A shear effect in a bending non-standard I-beam under uniformly distributed load

Ewa **Magnucka-Blandzi** [a, *] , Krzysztof **Magnucki** [b]

[a] *Institute of Mathematics, Poznan University of Technology, Poznan, Poland*
[b] *Łukasiewicz Research Network – Poznan Institute of Technology, 6 Ewarysta Estkowskiego St., 61-755 Poznań, Poland*

The paper is devoted to the analytical study of the bending problem of a simply supported or clamped non-standard I-beam under a uniformly distributed load. The cross-sectional shape of this beam, as a three-part structure, is analytically described. The purpose of this research is to present a detailed analytical model of this beam, considering the shear effect and its influence on the beam's deflection. This model is formulated according to linear elastic theory, and the deformation of a planar cross-section after the bending of this beam due to the shear effect is determined. Based on the principle of stationary potential energy, two differential equations of equilibrium are obtained. These equations are analytically solved, and the dimensionless shear effect function and the relative deflection of this beam are derived. Consequently, the maximum dimensionless relative deflection and the dimensionless coefficient of the shear effect are determined. Exemplary calculations are carried out for three selected non-standard I-beams of different lengths, demonstrating a significant influence of the shear effect on the deflections of short beams, especially clamped beams.

1. Introduction

The shear effect, especially in short beams, has a significant impact on their deflection. Wang et al. [20] described the development of the theory of the shear effect in beams and plates in the 20th century. They pointed, among others, to Timoshenko beam theory and generalization of the Euler-Bernoulli beam theory. A very intensive development of the theory of the shear effect in beams, plates and shells with various structures is evident in the 21st century. Ghugal and Sharma [5] elaborated the hyperbolic shear deformation theory for thick isotropic beam with rectangular cross section and analytically studied its bending under uniformly distributed load or three-point bending, as well as its free flexural vibration. Reddy [16] presented a reformulation of the classical and shear deformation theories for beams and plates, taking into account the constitutive relations of Eringen and the nonlinear strains of von Karman, and then formulated the equilibrium equations of beams and plates with an emphasis on improving finite element models. Akgöz

and Civalek [1] carried out an analytical studies of the static bending and free vibrations of simply supported microbeams by taking into account the developed higher-order shear strain theory based on the modified strain gradient theory. Bardella and Mattei [2] formulated an analytical model of a bending sandwich beam using the Jouravski method (Zhuravsky method) in order to accurately determine the shear stress distribution in the cross-sections of these beams. They carried out exemplary analytical and numerical FEM tests of such beams under uniformly distributed load. Sawant and Dahake [18] developed a new hyperbolic shear deformation theory for analysis of thick beams. This theory satisfies the necessary condition of zeroing the shear stresses on the top and bottom surfaces of the beam. Taking this theory into account, they analytically examined an example cantilever beam under load of varying distributed. Elishakoff et al. [3] presented in detail the simpler governing differential equation of Timoshenko beam theory, as well as comments in the context of other studies regarding this theory. Mahi et al. [15] presented a new theory of hyperbolic shear

---

* Corresponding author: ewa.magnucka-blandzi@put.poznan.pl (E. Magnucka-Blandzi)

deformation, indicating its application to the analysis of bending and free vibrations of isotropic, functionally graded sandwich and laminated composite plates. They compared the results of sample studies with those known from the literature. Thai et al. [19] described a simple beam theory taking into account the shear deformation effect with an indication of its application to the analysis of static bending and free vibration of isotropic nanobeams. Genovese and Elishakoff [4] pointed out the significance of the principle of virtual work, of the objectivity and of the energy balance in the formulation of planar static rod theories, in relation to a large deformations with consideration of the transverse shear effect. Magnucki [7] analytically described the bending of simply supported sandwich beams and I-beams of symmetrical structure. The analytical models of these beams were developed taking into account the classical "broken line" theory and nonlinear – polynomial theory. He pointed out the similarity of the sandwich structure to the I-beam structure. Magnucki et al. [8] studied analytically and numerically (FEM) the bending of beams with bisymmetrical cross sections under a generalized load. The analytical model of such a beam was developed taking into account the so-called the Zhuravsky shear stress formula. Magnucki and Witkowski [9] analyzed the problem of effective shaping of the bisymmetric cross-section of a bending beam based on the objective function regarding the maximum of the inertia moment and minimum of the area of this cross section, taking into account the condition limiting the maximum shear stresses. They presented effective shapes of the exemplary beams. Ren et al [17] proposed a new third-order zigzag model for asymmetric and symmetric laminated composite beams with emphasis on the new shear deformation function of the shear effect. They also presented analytical and numerical (FEM) solutions for the static analysis of laminated beams. They demonstrated the advantages of this model by comparing it with other classic theoretical models. Magnucki [10] investigated analytically the bending of homogeneous beams with bisymmetric cross-sections, three-layer beams and functionally graded beams, taking into account the individual theory of shear deformations of beams, using the classical formula for shear stress, called Zhuravsky shear stress. Magnucki and Magnucka-Blandzi [11] presented the problem of bending an asymmetric sandwich beam with one end simply supported and the other clamped end. They developed the analytical model of the beam taking into account the individual nonlinear deformation function of a planar beam cross section and carried out detailed tests for two example beams. The problems of bending, buckling and free flexural vibration of beams and plates demonstrated in the

above articles have been intensively analyzed and are published in the following recent works: Kustosz et al. [6], Magnucki and Sowiński [12], Magnucki et al. [13] and Magnucki [14]. A different problem, but very important for the structure, was presented by Ziemian and Ziemian [21]. They numerically investigated the problem of the impact of reduced strength of welded aluminum alloy beams and described in detail numerous variants of such I-beams.

The subject of the paper is homogeneous beam of length L and depth h with non-standard cross section I-beam (Fig. 1).
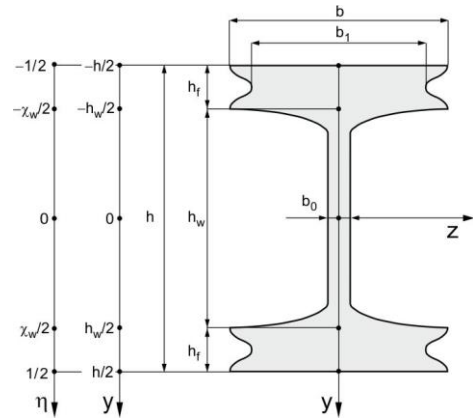

Fig. 1. Scheme of the cross section

The widths of the successive parts of this cross section are as follows:

- the upper flange $(-1/2 \leq \eta \leq -\chi_w/2)$

$$b(\eta) = bf_{uf}(\eta) \tag{1}$$

where

$$f_{uf}(\eta) = \beta_1 + (1 - \beta_1)\sin^2\left(\frac{\pi}{2}\frac{4\eta + 1 + \chi_w}{1 - \chi_w}\right) \tag{2}$$

- the web $(-\chi_w/2 \leq \eta \leq \chi_w/2)$

$$b(\eta) = bf_w(\eta) \tag{3}$$

where

$$f_w(\eta) = \beta_0 + (1 - \beta_0)\left(2\frac{\eta}{\chi_w}\right)^n \tag{4}$$

- the lower flange $(\chi_w/2 \leq \eta \leq 1/2)$

$$b(\eta) = bf_{lf}(\eta) \tag{5}$$

where

$$f_{lf}(\eta) = \beta_1 + (1 - \beta_1)\sin^2\left(\frac{\pi}{2}\frac{4\eta - 1 - \chi_w}{1 - \chi_w}\right) \tag{6}$$

and: $\eta = y/h$ – dimensionless coordinate, $\chi_w = h_w/h$, $\beta_1 = b_1/b$, $\beta_0 = b_0/b$ – dimensionless sizes, n – even exponent.

The main objective of this work is to develop an analytical model of this beam with consideration of the individual shear deformation theory and determine deflections of the simply supported and clamped beam.

2. Analytical model the beam

The analytical model of this beam is developed taking into account the papers [8, 10, 13] and [14]. Figure 2 shows a pictorial diagram of the deformation of the plane cross-section of this beam after bending.
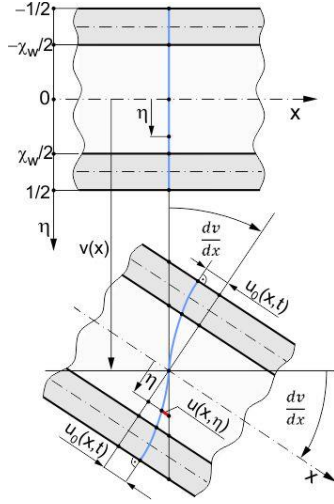

Fig. 2. Pictorial graph of the deformation of a plane cross-section

According to the presented diagram (Fig. 2), the longitudinal displacements for small deflections in the successive parts of the beam cross-section are written as follows:

- the upper flange ($-1/2 \le \eta \le -\chi_w/2$)

$$u^{(uf)}(x,\eta) = -h\left[\eta\frac{dv}{dx} - f_d^{(uf)}(\eta)\psi(x)\right] \qquad (7)$$

- the web ($-\chi_w/2 \le \eta \le \chi_w/2$)

$$u^{(w)}(x,\eta) = -h\left[\eta\frac{dv}{dx} - f_d^{(w)}(\eta)\psi(x)\right] \qquad (8)$$

- the lower flange ($\chi_w/2 \le \eta \le 1/2$)

$$u^{(lf)}(x,\eta) = -h\left[\eta\frac{dv}{dx} - f_d^{(lf)}\psi(\eta)(x)\right] \qquad (9)$$

where: $v(x)$ – deflection, $u_o(x)$ – longitudinal displacement on the outer surfaces, $\psi(x) = u_o(x)/h$ – dimensionless shear effect function, $f_d^{(uf)}(\eta)$, $f_d^{(w)}(\eta)$, $f_d^{(lf)}(\eta)$ – unknown dimensionless deformation functions.

Then, according to Hooke's law, the strains and stresses in each part are written in the following form:

- the upper flange ($-1/2 \le \eta \le -\chi_w/2$)

$$\varepsilon_x^{(uf)}(x,\eta) = -h\left[\eta\frac{d^2v}{dx^2} - f_d^{(uf)}(\eta)\frac{d\psi}{dx}\right] \qquad (10)$$

$$\gamma_{xy}^{(uf)}(x,\eta) = \frac{df_d^{(uf)}}{d\eta}\psi(x) \qquad (11)$$

$$\sigma_x^{(uf)}(x,\eta) = E\varepsilon_x^{(uf)}(x,\eta) \qquad (12)$$

$$\tau_{xy}^{(uf)}(x,\eta) = \frac{E}{2(1+\nu)}\gamma_{xy}^{(uf)}(x,\eta) \qquad (13)$$

- the web ($-\chi_w/2 \le \eta \le \chi_w/2$)

$$\varepsilon_x^{(w)}(x,\eta) = -h\left[\eta\frac{d^2v}{dx^2} - f_d^{(w)}(\eta)\frac{d\psi}{dx}\right] \qquad (14)$$

$$\gamma_{xy}^{(w)}(x,\eta) = \frac{df_d^{(w)}}{d\eta}\psi(x) \qquad (15)$$

$$\sigma_x^{(w)}(x,\eta) = E\varepsilon_x^{(w)}(x,\eta) \qquad (16)$$

$$\tau_{xy}^{(w)}(x,\eta) = \frac{E}{2(1+\nu)}\gamma_{xy}^{(w)}(x,\eta) \qquad (17)$$

- the lower flange ($\chi_w/2 \le \eta \le 1/2$)

$$\varepsilon_x^{(lf)}(x,\eta) = -h\left[\eta\frac{d^2v}{dx^2} - f_d^{(lf)}(\eta)\frac{d\psi}{dx}\right] \qquad (18)$$

$$\gamma_{xy}^{(lf)}(x,\eta) = \frac{df_d^{(lf)}}{d\eta}\psi(x) \qquad (19)$$

$$\sigma_x^{(lf)}(x,\eta) = E\varepsilon_x^{(lf)}(x,\eta) \qquad (20)$$

$$\tau_{xy}^{(lf)}(x,\eta) = \frac{E}{2(1+\nu)}\gamma_{xy}^{(lf)}(x,\eta) \qquad (21)$$

where: E – Young's module, ν – Poisson ratio.

The unknown dimensionless deformation functions in successive parts of the cross section are determined analytically as follows:

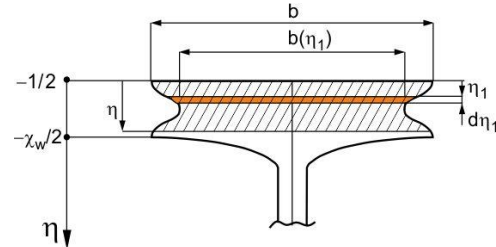- the upper flange ($-1/2 \le \eta \le -\chi_w/2$)

Fig. 3. Hatched cross-section area of selected beam part

According to the above figure (Fig. 3), the dimensionless first moment of the hatched area is written as follows

$$\bar{S}_z^{(uf)}(\eta) = -\int_{-1/2}^{\eta}\eta_1 f_{uf}(\eta_1)d\eta_1 \qquad (22)$$

The dimensionless deformation function

$$\frac{df_d^{(uf)}}{d\eta} = \frac{\bar{S}_z^{(uf)}(\eta)}{f_{uf}(\eta)} \qquad (23)$$

$$f_d^{(uf)}(\eta) = -C_f + \int_{-\chi_w/2}^{\eta}\frac{\bar{S}_z^{(uf)}(\eta)}{f_{uf}(\eta)}d\eta \qquad (24)$$

where

$$C_f = \int_0^{\chi_w/2}\frac{\bar{S}_z^{(w)}(\eta)}{f_w(\eta)}d\eta \qquad (25)$$

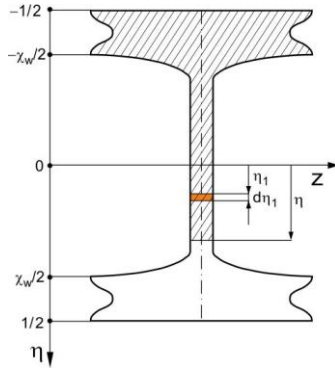- the web ($-\chi_w/2 \le \eta \le \chi_w/2$)

Fig. 4. Hatched cross-section area of selected beam part

According to the Fig. 4, the dimensionless first moment of the hatched region is written as follows

$$\bar{S}_z^{(w)}(\eta) = C_{zf} - \int_{-\chi_w/2}^{\eta} \eta_1 f_w(\eta_1) d\eta_1 \tag{26}$$

where

$$C_{zf} = - \int_{-1/2}^{-\chi_w/2} \eta f_{uf}(\eta) \, d\eta \tag{27}$$

The dimensionless deformation function

$$\frac{df_d^{(w)}}{d\eta} = \frac{\bar{S}_z^{(w)}(\eta)}{f_w(\eta)} \tag{28}$$

$$f_d^{(w)}(\eta) = \int \frac{\bar{S}_z^{(w)}(\eta)}{f_w(\eta)} d\eta \tag{29}$$

- the lower flange ($\chi_w/2 \le \eta \le 1/2$)

Consequently, the dimensionless first moment

$$\bar{S}_z^{(lf)}(\eta) = - \int_{1/2}^{\eta} \eta_1 f_{lf}(\eta_1) d\eta_1 \tag{30}$$

and the dimensionless deformation function

$$\frac{df_d^{(lf)}}{d\eta} = \frac{\bar{S}_z^{(lf)}(\eta)}{f_{lf}(\eta)} \tag{31}$$

$$f_d^{(lf)}(\eta) = C_f + \int_{\chi_w/2}^{\eta} \frac{\bar{S}_z^{(lf)}(\eta)}{f_{lf}(\eta)} d\eta \tag{32}$$

Based on the principle of stationary total potential energy $\delta(U_{\varepsilon,\gamma} - W) = 0$, after a simple transformation we obtain a system of two equilibrium differential equations in the following form:

$$\bar{J}_z \frac{d^2 v}{dx^2} - C_{v\psi} \frac{d\psi}{dx} = - \frac{M_b(x)}{Ebh^3} \tag{33}$$

$$C_{v\psi} \frac{d^3 v}{dx^3} - C_{\psi\psi} \frac{d^2\psi}{dx^2} + C_\psi \frac{\psi(x)}{h^2} = 0 \tag{34}$$

where: $M_b(x)$ – the bending moment, and dimensionless coefficients

$$\bar{J}_z = \bar{J}_{z1} + \bar{J}_{z2} + \bar{J}_{z3} \tag{35}$$

where

$$\bar{J}_{z1} = \int_{-1/2}^{-\chi_w/2} \eta^2 f_{uf}(\eta) d\eta, \quad \bar{J}_{z2} = \int_{-\chi_2/2}^{\chi_w/2} \eta^2 f_w(\eta) d\eta,$$

$$\bar{J}_{z3} = \int_{\chi_2/2}^{1/2} \eta^2 f_{lf}(\eta) d\eta$$

$$C_{v\psi} = C_{v\psi1} + C_{v\psi2} + C_{v\psi3} \tag{36}$$

where

$$C_{v\psi1} = \int_{-1/2}^{-\chi_w/2} \eta f_d^{(uf)}(\eta) f_{uf}(\eta) d\eta$$

$$C_{v\psi2} = \int_{-\chi_2/2}^{\chi_w/2} \eta f_d^{(w)}(\eta) f_w(\eta) d\eta$$

$$C_{v\psi3} = \int_{\chi_2/2}^{1/2} \eta f_d^{(lf)}(\eta) f_{lf}(\eta) d\eta$$

$$C_{\psi\psi} = C_{\psi\psi1} + C_{\psi\psi2} + C_{\psi\psi3} \tag{37}$$

where

$$C_{\psi\psi1} = \int_{-1/2}^{-\chi_w/2} \left[f_d^{(uf)}(\eta) \right]^2 f_{uf}(\eta) d\eta$$

$$C_{\psi\psi2} = \int_{-\chi_2/2}^{\chi_w/2} \left[f_d^{(w)}(\eta) \right]^2 f_w(\eta) d\eta$$

$$C_{\psi\psi3} = \int_{\chi_2/2}^{1/2} \left[f_d^{(lf)}(\eta) \right]^2 f_{lf}(\eta) d\eta$$

$$C_\psi = \frac{1}{2(1+\nu)} \left(C_{\psi1} + C_{\psi2} + C_{\psi3} \right) \tag{38}$$

where

$$C_{\psi1} = \int_{-1/2}^{-\chi_w/2} \left[df_d^{(uf)}/d\eta \right]^2 f_{uf}(\eta) d\eta$$

$$C_{\psi2} = \int_{-\chi_2/2}^{\chi_w/2} \left[df_d^{(w)}/d\eta \right]^2 f_w(\eta) d\eta$$

$$C_{\psi3} = \int_{\chi_2/2}^{1/2} \left[df_d^{(lf)}/d\eta \right]^2 f_{lf}(\eta) d\eta$$

Two differential equations of equilibrium (33) and (34), after simply transformations, are as follows:

$$\bar{J}_z \frac{d^2\bar{v}}{d\xi^2} - C_{v\psi} \frac{d\psi}{d\xi} = - \lambda \frac{M_b(\xi)}{Ebh^2} \tag{39}$$

$$\frac{d^2\psi}{d\xi^2} - (\alpha\lambda)^2 \psi(\xi) = - \frac{C_{v\psi}}{\bar{J}_z C_{\psi\psi} - C_{v\psi}^2} \lambda^2 \frac{T(\xi)}{Ebh} \tag{40}$$

where: $\xi = x/L$ – dimensionless coordinate, $\lambda = L/h$ – relative length, $\bar{v}(\xi) = v(\xi)/L$ – relative deflection, and dimensionless coefficient

$$\alpha = \sqrt{\frac{\bar{J}_z C_\psi}{\bar{J}_z C_{\psi\psi} - C_{v\psi}^2}} \tag{41}$$

These equations (39) and (40) are convenient for further detailed research of beams.

3. Analytical bending study of the beam

3.1. Simply supported beam

The simply supported beam under uniformly distributed load of intensity q [N/mm] is shown in Fig.5.
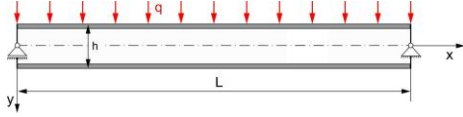
Fig. 5. Scheme of the simply supported beam

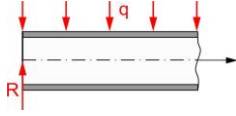The scheme of the left part of this beam with load q and reaction force R is shown in Fig. 6.

Fig. 6. Scheme of the left part of this beam

Therefore, according to the above scheme, the reaction R = qL/2, also the shear force $T(\xi)$ and bending moment $M_b(\xi)$ are as follows:

$$T(\xi) = \frac{1}{2}(1 - 2\xi)qL \qquad (42)$$

$$M_b(\xi) = \frac{1}{2}(\xi - \xi^2)qL^2 \qquad (43)$$

Substituting above expressions (42) and (43) into these equilibrium equations (39) and (40), after simply transformations, one obtains:

• the dimensionless shear effect function

$$\psi_s(\xi) = \overline{\psi}_s(\xi)\frac{q}{Eb} \qquad (44)$$

where

$$\overline{\psi}_s(\xi) = \frac{1}{2}\left\{1 - 2\xi - 2\frac{\sinh[(0.5-\xi)\alpha\lambda]}{\alpha\lambda\cosh(0.5\alpha\lambda)}\right\}\frac{C_{v\psi}}{\overline{J}_z C_\psi}\lambda \qquad (45)$$

• the relative deflection

$$\overline{v}_s(\xi) = \tilde{v}_s(\xi)\frac{q}{Eb} \qquad (46)$$

where

$$\tilde{v}_s(\xi) = \frac{1}{24}\left[(1 - 2\xi^2 + \xi^3)\xi + f_\psi^{(s)}(\xi)\frac{C_{v\psi}^2}{\overline{J}_z C_\psi}\frac{1}{\lambda^2}\right]\frac{\lambda^3}{\overline{J}_z} \qquad (47)$$

and

$$f_\psi^{(s)}(\xi) = 12 \cdot$$
$$\cdot \left\{(1 - \xi)\xi - 2\frac{\cosh(0.5\alpha\lambda) - \cosh[(0.5-\xi)\alpha\lambda]}{(\alpha\lambda)^2\cosh(0.5\alpha\lambda)}\right\} \qquad (48)$$

These functions (45) and (47) satisfies the following conditions: $(d\overline{\psi}_s/d\xi)_0 = (d\overline{\psi}_s/d\xi)_1 = 0$, $\overline{\psi}_s(1/2) = 0$, $\tilde{v}_s(0) = \tilde{v}_s(1) = 0$, $(d\tilde{v}_s/d\xi)_{1/2} = 0$.

The maximum of the function (45)

$$\overline{\psi}_{s,max} = \overline{\psi}_s(0) = \frac{1}{2}\left\{1 - 2\frac{\tanh(0.5\alpha\lambda)}{\alpha\lambda}\right\}\frac{C_{v\psi}}{\overline{J}_z C_\psi}\lambda \qquad (49)$$

The maximum of the dimensionless relative deflection (47) is as follows

$$\tilde{v}_{s,max} = \tilde{v}_s\left(\frac{1}{2}\right) = \left(1 + C_{se}^{(s)}\right)\frac{5\lambda^3}{384\overline{J}_z} \qquad (50)$$

and the dimensionless coefficient of the shear effect

$$C_{se}^{(s)} = \frac{48}{5\lambda^2}\left[1 - 8\frac{\cosh(0.5\alpha\lambda) - 1}{(\alpha\lambda)^2\cosh(0.5\alpha\lambda)}\right]\frac{C_{v\psi}^2}{\overline{J}_z C_\psi} \qquad (51)$$

3.2. Clamped beam

The clamped beam under uniformly distributed load of intensity q [N/mm] is shown in Fig. 7.
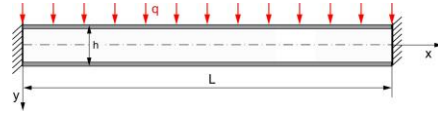

Fig. 7. Scheme of the clamped beam

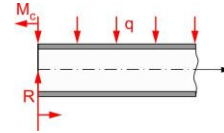The scheme of the left part of this beam with load q, two reactions (force R and moment M_c) is shown in Fig. 8.

Fig. 8. Scheme of the left part of this beam

Therefore, according to the above scheme, the reactions R = qL/2 and M_c,

• the shear force

$$T(\xi) = \frac{1}{2}(1 - 2\xi)qL \qquad (52)$$

• bending moment

$$M_b(\xi) = \frac{1}{2}(\xi - \xi^2 - 2\overline{M}_c)qL^2 \qquad (53)$$

where: $\overline{M}_c = M_c/qL^2$ – dimensionless reaction moment.

Substituting above expressions (52) and (53) into these equilibrium equations (39) and (40), after simply transformations, one obtains:

• the dimensionless shear effect function

$$\psi_c(\xi) = \overline{\psi}_c(\xi)\frac{q}{Eb} \qquad (54)$$

where

$$\overline{\psi}_c(\xi) = \frac{1}{2}\left\{1 - 2\xi - \frac{\sinh[(0.5-\xi)\alpha\lambda]}{\sinh(0.5\alpha\lambda)}\right\}\frac{C_{v\psi}}{\overline{J}_z C_\psi}\lambda \qquad (55)$$

• the relative deflection

$$\overline{v}_c(\xi) = \tilde{v}_c(\xi)\frac{q}{Eb} \qquad (56)$$

where

$$\tilde{v}_c(\xi) = \frac{1}{24}\left[(1 - \xi)^2\xi^2 + f_\psi^{(c)}(\xi)\frac{C_{v\psi}^2}{\overline{J}_z C_\psi}\frac{1}{\lambda^2}\right]\frac{\lambda^3}{\overline{J}_z} \qquad (57)$$

and

$$f_\psi^{(c)}(\xi) = 12 \cdot$$

$$\cdot \left\{ (1-\xi)\xi - 2\frac{\cosh(0.5\alpha\lambda) - \cosh[(0.5-\xi)\alpha\lambda]}{\alpha\lambda \sinh(0.5\alpha\lambda)} \right\} \quad (58)$$

These functions (55) and (57) satisfies the following conditions: $\overline{\psi}_c(0) = \overline{\psi}_c(1/2) = \overline{\psi}_c(1) = 0$, $(d\tilde{v}_s/d\xi)_0 = (d\tilde{v}_s/d\xi)_{1/2} = (d\tilde{v}_s/d\xi)_1 = 0$, $\tilde{v}_s(0) = \tilde{v}_s(1) = 0$, and from which $\overline{M}_c = 1/12$.

The maximum of the function (55)

$$\overline{\psi}_{c,max} = \overline{\psi}_c(\xi_e) \quad (59)$$

where the dimensionless coordinate value ξ_e is calculated from the condition $d\overline{\psi}_c/d\xi = 0$.

The maximum of the dimensionless relative deflection (57)

$$\tilde{v}_{c,max} = \tilde{v}_c\left(\frac{1}{2}\right) = \left(1 + C_{se}^{(c)}\right)\frac{\lambda^3}{384\bar{J}_z} \quad (60)$$

and the dimensionless coefficient of the shear effect

$$C_{se}^{(c)} = \frac{48}{\lambda^2}\left[1 - 4\frac{\cosh(0.5\alpha\lambda) - 1}{\alpha\lambda\sinh(0.5\alpha\lambda)}\right]\frac{C_{v\psi}^2}{\bar{J}_z C_\psi} \quad (61)$$

4. Detailed bending studies of exemplary beams

Detailed tests were performed for three exemplary beams:
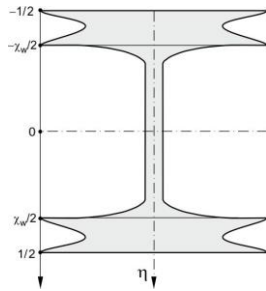
- the first beam B-1 (Fig. 9)

Fig. 9. Scheme of the cross section of this beam

The dimensionless sizes of this beam: $\chi_w = 5/7$, $\beta_0 = 1/12$, $\beta_1 = 0.6$, $n = 20$, $\nu = 0.3$.

The shape of deformation of the planar cross section of this beam: functions $f_d(\eta)$ – expressions (24), (29), (32), and its derivatives $df_d/d\eta$ – expressions (23), (28), (31) are shown in Fig. 10.

Graphs of the dimensionless shear effect function (45) and the relative deflection (47) for the simply supported beam (Subsection 3.1, Fig. 5) are shown in Fig. 11.
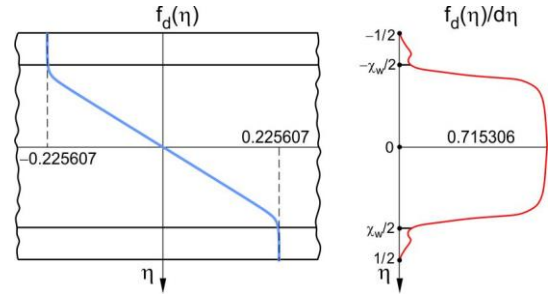

Fig. 10. Graphs of deformation functions $f_d(\eta)$ and its derivatives $df_d/d\eta$ of this beam
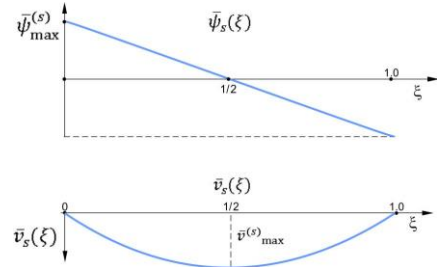

Fig. 11. Graphs of the dimensionless shear effect function (45) and the relative deflection (47) of the simply supported beam

Graphs of the dimensionless shear effect function (55) and the relative deflection (57) for the clamped beam (Subsection 3.2, Fig. 7) are shown in Fig. 12.
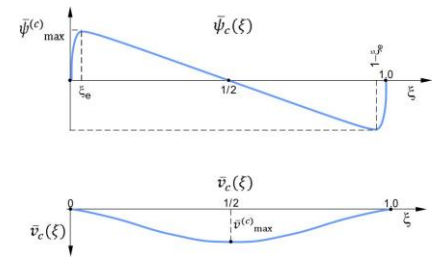

Fig. 12. Graphs of the dimensionless shear effect function (55) and the relative deflection (57) of the clamped beam

The selected results of detailed calculations are as follows: the values of the maximum of the dimensionless shear effect function $\overline{\psi}_{s,max}$ (49), the dimensionless coefficient of the shear effect $C_{se}^{(s)}$ (51) and the maximum of the dimensionless relative deflection $\tilde{v}_{s,max}$ (50) for the simply supported beam of relative lengths $\lambda = 5, 10, 15$, are specified in Table 1.

Table 1. Selected values of calculations for simply supported beam B-1

λ	5	10	15
$\overline{\psi}_{s,max}$	125.841	259.608	393.374
$C_{se}^{(s)}$	0.530321	0.133285	0.0592956
$\tilde{v}_{s,max}$	51.259	303.677	957.995

Also, above selected values $\overline{\psi}_{c,max}$ (59), $C_{se}^{(c)}$ (61) and $\tilde{v}_{c,max}$ (60) for the clamped this beam are specified in Table 2.

Table 2. Selected values of calculations for clamped beam B-1

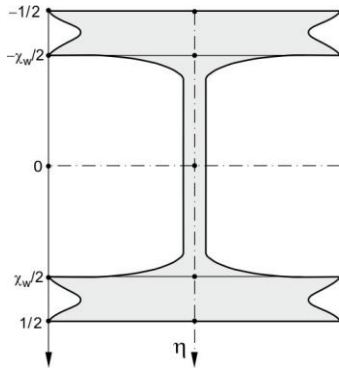| λ	5	10	15
ξ_e	0.0837145	0.0521235	0.0387526
$\bar{\psi}_{c,max}$	103.445	231.718	362.271
$C_{se}^{(c)}$	2.35398	0.628046	0.284991
$\tilde{v}_{c,max}$	22.468	87.251	232.421

- the second beam B-2 (Fig. 13)

Fig. 13. Scheme of the cross section of this beam

The dimensionless sizes of this beam: $\chi_w = 5/7$, $\beta_0 = 1/12$, $\beta_1 = 0.8$, n = 20, $\nu = 0.3$.

The shape of deformation of the planar cross section of this beam: functions $f_d(\eta)$ – expressions (24), (29), (32), and its derivatives $df_d/d\eta$ – expressions (23), (28), (31) are shown in Fig. 14.
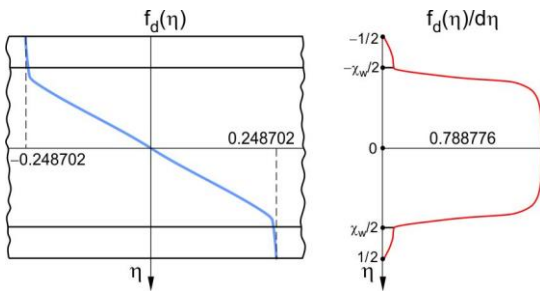

Fig. 14. Graphs of deformation functions $f_d(\eta)$ and its derivatives $df_d/d\eta$ of this beam

Graphs of the dimensionless shear effect function (45), (55) and the relative deflection (47), (57) for the simply supported beam (Subsection 3.1, Fig. 5) and the clamped beam (Subsection 3.2, Fig. 7) are similar to the graphs shown in Fig. 11 and Fig. 12. Thus, the results of the detailed calculations for this beam are specified in Tables 3 and 4.

Table 3. Selected values of calculations for simply supported beam B-2

λ	5	10	15
$\bar{\psi}_{s,max}$	113.398	234.083	354.769
$C_{se}^{(s)}$	0.583770	0.146746	0.0652868
$\tilde{v}_{s,max}$	47.861	277.235	869.201

Table 4. Selected values of calculations for clamped beam B-2

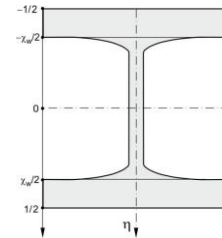| λ	5	10	15
ξ_e	0.0847480	0.0528374	0.0393054
$\bar{\psi}_{c,max}$	92.942	208.577	326.307
$C_{se}^{(c)}$	2.585209	0.690687	0.313548
$\tilde{v}_{c,max}$	21.669	81.747	214.353

- the third beam B-3 (Fig. 15)

Fig. 15. Scheme of the cross section of this beam

The dimensionless sizes of this beam: $\chi_w = 5/7$, $\beta_0 = 1/12$, $\beta_1 = 1.0$, n = 20, $\nu = 0.3$.

The results of the detailed calculations for this beam, similarly to beams B-1 and B-2, are presented graphically in Fig. 16 and specified in Table 5 and 6.
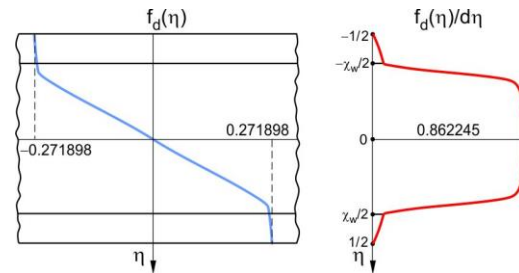

Fig. 16. Graphs of deformation functions $f_d(\eta)$ and its derivatives $df_d/d\eta$ of this beam

Table 5. Selected values of calculations for simply supported beam B-3

λ	5	10	15
$\bar{\psi}_{s,max}$	103.188	213.123	323.058
$C_{se}^{(s)}$	0.637308	0.160234	0.0712897
$\tilde{v}_{s,max}$	45.071	255.509	796.235

Table 6. Selected values of calculations for clamped beam B-3

λ	5	10	15
ξ_e	0.0856342	0.0534512	0.0397812
$\bar{\psi}_{c,max}$	84.360	189.619	296.818
$C_{se}^{(c)}$	2.816657	0.753423	0.342152
$\tilde{v}_{c,max}$	21.013	77.228	199.511

5. Conclusions

Taking into account the analytical tests of beam bending with the shear effect taken into account, the following remarks were made:
a) the shear effect in bending beams, expressed by the coefficients $C_{se}^{(s)}$ (51) and $C_{se}^{(c)}$ (61), increases their deflection

b) the values of coefficients (51) and (61) decrease with the increase of the relative length λ of these beams, therefore in the case of long beams the shear effect is negligible

c) the shear effect in bending short beams is dominant, significantly increasing their deflection, especially in clamped beams

d) the presented algorithm for analytical modeling of a selected beam can be used for beams with other cross sections, as well as for functionally graded beams.

Bibliography

[1] Akgöz B, Civalek Ö. A size-dependent shear deformation beam model based on the strain gradient elasticity theory. Int J Eng Sci. 2013;70:1-14. https://doi.org/10.1016/j.ijengsci.2013.04.004

[2] Bardella L, Mattei O. On explicit analytic solutions for the accurate evaluation of the shear stress in sandwich beams with a clamped end. Compos Struct. 2014;112:157-168. https://doi.org/10.1016/j.compstruct.2014.01.044

[3] Elishakoff I, Kaplunov J, Nolde E. Celebrating the centenary of Thimoshenko's study of effects of shear deformation and rotary inertia. Appl Mech Rev. 2015; 67:060802. https://doi.org/10.1115/1.4031965

[4] Genovese D, Elishakoff I. Shear deformable rod theories and fundamental principles of mechanics. Arch Appl Mech. 2019;89:1995-2003. https://doi.org/10.1007/s00419-019-01556-7

[5] Ghugal YM, Sharma R. A hyperbolic shear deformation theory for flexure and vibration of thick isotropic beams. Int J Comput Methods. 2009;6(4):585-604. https://doi.org/10.1142/S0219876209002017

[6] Kustosz J, Magnucki K, Goliwąs D. Strength of a bent sandwich beam with clamped ends. Rail Vehicles/ Pojazdy Szynowe. 2023;1-2:3-7. https://doi.org/10.53502/RAIL-161868

[7] Magnucki K. Bending of symmetrically sandwich beams and I-beams – analytical study. Int J Mech Sci. 2019;150:411-419. https://doi.org/10.1016/j.ijmecsci.2018.10.020

[8] Magnucki K, Lewinski J, Magnucka-Blandzi E. A shear deformation theory of beams with bisymmetrical cross-section based on the Zhuravsky shear stress formula. Engineering Transactions. 2020;68(4):353-370. https://doi.org/10.24423/EngTrans.1174.20201120

[9] Magnucki K, Witkowski D. Effective shaping of a bisymmetrical cross section of beams under shear stresses constraints. IOP Conf Ser: Mater Sci Eng. 2021;1199:012062. https://doi.org/10.1088/1757-899X/1199/1/012062

[10] Magnucki K. An individual shear deformation theory of beams with consideration of the Zhuravsky shear stress formula. In: Zingoni A (ed.). Current Perspectives and New Directions in Mechanics, Modelling and Design of Structural Systems, CRC Press, Taylor & Francis Group, Boca Raton, London, New York 2022;682-689. https://doi.org/10.1201/9781003348443-112

[11] Magnucki K, Magnucka-Blandzi E. A refined shear deformation theory of an asymmetric sandwich beam with porous core: linear bending problem. Appl Math Model. 2023;124:624-638. https://doi.org/10.1016/j.apm.2023.08.025

[12] Magnucki K, Sowiński K. Bending of a sandwich beam with an individual functionally graded core. J Theor App Mech. 2024;62(1):3-17. https://doi.org/10.15632/jtam-pl/174698

[13] Magnucki K, Magnucka-Blandzi E, Witkowski D, Stefańska N. Bending of a homogeneous beam with a monosymmetric cross section – shear effect. Engineering Transactions. 2024;72(3):285-307. https://doi.org/10.24423/EngTrans.2024.3242

[14] Magnucki K. Free flexural vibrations of standard wide-flange H-beams with consideration of the shear effect. Rail Vehicles/Pojazdy Szynowe. 2024;1-2:46-50. https://doi.org/10.53502/RAIL-189244

[15] Mahi A, Bedia EAA, Tounsi A. A new hyperbolic shear deformation theory for bending and free vibration analysis of isotropic, functionally graded, sandwich and laminated composite plates. Appl Math Model. 2015;39:2489-2508. https://doi.org/10.1016/j.apm.2014.10.045

[16] Reddy JN. Nonlocal nonlinear formulations for bending of classical and shear deformation theories of beams and plates. Int J Eng Sci. 2010;48:1507-1518. https://doi.org/10.1016/j.ijengsci.2010.09.020

[17] Ren S, Cheng C, Meng Z, Yu B, Zhao G. A new general third-order zigzag model for asymmetric and symmetric laminated composite beams. Compos Struct. 2021;260:113523. https://doi.org/10.1016/j.compstruct.2020.113523

[18] Sawant M, Dahake AG. A new hyperbolic shear deformation theory for analysis of thick beam. International Journal of Innovative Research in Science, Engineering and Technology. 2014;3(2):9636-9643. https://www.researchgate.net/publication/260366415

[19] Thai S, Thai H-T, Vo TP, Patel VI. A simple shear deformation theory for nonlocal beams. Compos Struct. 2018;183:262-270. https://doi.org/10.1016/j.compstruct.2017.03.022

[20] Wang CM, Reddy JN, Lee KH. Shear deformable beams and plates. Relationships with classical solutions. Elsevier: Amsterdam, New York, Tokyo 2000.

[21] Ziemian CW, Ziemian RD. Numerical investigation of the influence of transverse welds on the strength of aluminum alloy I-shape members – beams. Structures. 2024;60:105861. https://doi.org/10.1016/j.istruc.2024.105861